In Vitro Metabonomic Study Detects Increases in UDP-GlcNAc and UDP-GalNAc, as Early Phase Markers of Cisplatin Treatment Response in Brain Tumor Cells

ARTICLE *in* JOURNAL OF PROTEOME RESEARCH · JUNE 2011

Impact Factor: 4.25 · DOI: 10.1021/pr200114v · Source: PubMed

8 AUTHORS, INCLUDING:

Martin Wilson
University of Birmingham
45 PUBLICATIONS **451** CITATIONS
SEE PROFILE

Theodoros Arvanitis
The University of Warwick
191 PUBLICATIONS **1,474** CITATIONS
SEE PROFILE

Journal of proteome research

ARTICLE

pubs.acs.org/jpr

In Vitro Metabonomic Study Detects Increases in UDP-GlcNAc and UDP-GalNAc, as Early Phase Markers of Cisplatin Treatment Response in Brain Tumor Cells

Xiaoyan Pan,[†,‡] Martin Wilson,[†,‡] Ladan Mirbahai,[§] Carmel McConville,[†] Theodoros N. Arvanitis,[‡,∥] Julian L. Griffin,[⊥] Risto A. Kauppinen,[#,¶] and Andrew C. Peet*[,†,‡,¶]

[†]Cancer Sciences, University of Birmingham, Birmingham, United Kingdom

[‡]Birmingham Children's Hospital NHS Foundation Trust, Birmingham, United Kingdom

[§]Sports and Exercise Science, University of Birmingham, Birmingham, United Kingdom

[∥]Electronic, Electrical and Computer Engineering, University of Birmingham, Birmingham, United Kingdom

[⊥]Department of Biochemistry, University of Cambridge, Cambridge, United Kingdom

[#]Clinical Research and Imaging Centre, Department of Experimental Psychology, University of Bristol, Bristol, United Kingdom

Supporting Information

ABSTRACT: O-linked β-*N*-acetylglucosamine glycosylation (O-GlcNAcylation) is important in a number of biological processes and diseases including transcription, cell stress, diabetes, and neurodegeneration and may be a marker of tumor metastasis. Uridine diphospho-*N*-acetylglucosamine (UDP-GlcNAc), the donor molecule in O-GlcNAcylation, can be detected by ^{1}H nuclear magnetic resonance spectroscopy (^{1}H NMR), giving the potential to measure its level noninvasively, providing a novel biomarker of prognosis and treatment monitoring. In this in vitro metabonomic study, four brain cancer cell lines were exposed to cisplatin and studied for metabolic responses using ^{1}H NMR. The Alamar blue assay and DAPI staining were used to assess cell sensitivity to cisplatin treatment and to confirm cell death. It is shown that in the cisplatin responding cells, UDP-GlcNAc and uridine diphospho-*N*-acetylgalactosamine (UDP-GalNAc), in parallel with ^{1}H NMR detected lipids, increased with cisplatin exposure before or at the onset of the microscopic signs of evolving cell death. The changes in UDP-GlcNAc and UDP-GalNAc were not detected in the nonresponders. These glycosylated UDP compounds, the key substrates for glycosylation of proteins and lipids, are commonly implicated in cancer proliferation and malignant transformation. However, the present study mechanistically links UDP-GlcNAc and UDP-GalNAc to cancer cell death following chemotherapeutic treatment.

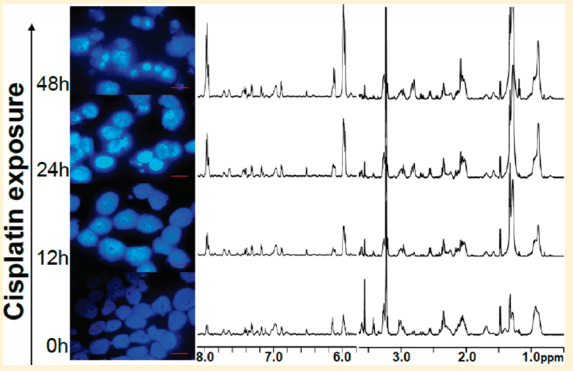

KEYWORDS: UDP-GlcNA, UDP-GalNAc, cisplatin, cell death, ^{1}H NMR, metabolomics

INTRODUCTION

O-linked β-*N*-acetylglucosamine glycosylation (O-GlcNAcylation) is the post-translational glycosylation of proteins with O-linked β-*N*-acetylglucosamine (O-GlcNAc),[1] with around 1000 such modified proteins being identified to date.[2,3] O-GlcNAcylation has been shown to be important in a number of biological processes and diseases including cell stress,[4] transcription,[5] diabetes[6] and neurodegeneration.[7] However, few studies have investigated the role of O-GlcNAcylation in cancer progression and treatment, but a recent report demonstrates an increase in O-GlcNAcylation in breast tumor metastasis compared with their primary tissues, suggesting that O-GlcNAcylation may be a potential target for therapeutic agents.[8]

The biosynthesis of O-GlcNAc begins with intracellular glucose, with 2−5% entering the hexosamine biosynthesis pathway (HBP). The direct donor of O-GlcNAc is UDP-*N*-acetylglucosamine (UDP-GlcNAc).[9] Recently the detection of molecules in the HBP by ^{1}H magnetic resonance spectroscopy(^{1}H NMR), including UDP-GlcNAc and UDP-GalNAc has been demonstrated from liver tissues[10] and intact tumor cells.[11] In addition to UDP-GlcNAc, ^{1}H NMR metabonomics/metabolomics can detect a number of metabolites in a untargeted fashion and identify new biomarkers[12] that have been shown to change in response to cell growth arrest[13] or early events of cell death,[14] making this a promising technique for monitoring cancer cell treatment.

^{1}H NMR has been shown to be a powerful method for detecting metabolite and lipid changes related to cell growth

Received: February 11, 2011

arrest and death both in vitro and in vivo. The most widely studied metabolites in this context are choline containing metabolites (CCMs) and lactate. Decreases in phosphocholine (PC) and increases in glycerophosphocholine (GPC) have been observed in apoptotic rat glioma, human breast cancer and leukemia cells induced by various drugs.[14−16] Similarly, reduced levels of PC were detected in HSV-tk gene therapy treated BT4C glioma cells leading to arrest in the G2/M phase of the cell cycle[17] and TNF-α treated breast cancer cells arrested in the G0/G1+S phase.[18] However, the concentrations of PC and GPC undergo changes during cell proliferation[19] complicating interpretation of cell status from these CCMs, and Tiechert and colleagues observed a decrease in the ratio of PC to GPC in prostate tumors.[20] Lactate has been shown to increase in human colon adenocarcinoma cells treated with TNF-α /IFN-γ[21] and has also been shown to decrease in neutrophils treated with TNF-α in vitro[22] and 5-fluorouracil treated fibrosarcoma in vivo.[23] These observations reflect the involvement of glycolysis, and hence the production of lactate, for the production of ATP in cells with a high proliferative capability as well as during the cell death process. In addition to CCM and lactate, using a metabonomic approach, a number of ^{1}H NMR detectable metabolites including taurine, glycine, alanine, succinate and glutamate have been observed to undergo changes in cisplatin treated apoptotic BT4C cells,[13] although UDP-GlcNAc and UDP-GalNAc were not assigned in this study. A number of endogenous metabolites yet to be identified may have potential for treatment monitoring by ^{1}H NMR.

Particular attention has also been paid to ^{1}H NMR detected lipids as spectroscopic and imaging biomarkers for cancer treatment response. ^{1}H NMR-observable lipids are often prominent in malignant tumors, in some cases reflecting hypoxia.[24] In addition, in response to cytotoxic treatment, both saturated and unsaturated lipids have been shown to increase in responding tumors.[17,25,26] Accumulation of ^{1}H NMR visible lipids has been demonstrated in apoptotic cells[27,28] and tumors in vivo[25] and has been correlated with the increase in cytoplasmic lipid droplets.[17,29]

In the present study, we have examined ^{1}H NMR metabolite profiles of two glioma and two neural tumor cell lines, with differing sensitivities to cisplatin. Cell death was assessed with Alamar Blue and DAPI-staining. We show that in the responding cells, UDP-GlcNAc and UDP-GalNAc, in parallel with ^{1}H NMR detected lipids, increase with cisplatin exposure before or at the onset of the microscopic signs of evolving cell death. To the authors' knowledge, this study is the first to report the concentration of UDP-N-acetylglucosamine in intact tumor cells exposed to a chemotherapeutic agent.

MATERIALS AND METHODS

Cell Culture and Harvest

BT4C, rat glioblastoma, U87-MG, human glioblastoma, DAOY, human medulloblastoma and PFSK-1, human supratentorial primitive neuroectodermal tumor (ST-PNET) cell lines were cultured in 75 cm^2 flasks with filter-vented caps (Corning, U.K.) and maintained in 15 mL Dulbecco's modified Eagles medium (DMEM F:12), with L-glutamine (GIBCO, Invitrogen Corporation, U.K.) supplemented with 10% (v/v) fetal calf serum (PAA, U.K.), 1% 200 mM L-glutamine (100×) (GIBCO, Invitrogen Corporation, U.K.), and 1% MEM nonessential amino acid solution (100×) (Sigma Aldrich, U.K.). The cells were incubated at 37 °C in a humidified atmosphere (5% CO_2, 95% air) and harvested at around 90% confluence. After washing with 10 mL ice-cold phosphate buffered saline (Invitrogen Ltd., Paisley, U.K.) three times, cells were then removed from the flask using a rubber policeman and centrifuged to form a pellet. Samples for high-resolution magic angle spinning ^{1}H NMR (HR-MAS) and metabolite extraction were snap-frozen in liquid nitrogen and stored at −80 °C.

Cisplatin Exposure

Ten to 100 μM Cisplatin (Sigma Aldrich, U.K.) working solution was freshly made from a stock solution with culture media before adding to the cell culture. Cells were harvested at the indicated time points.

Alamar Blue Assay for Cell Viability

Cells were seeded in flat-bottomed IWAKI 96-well culture plates at a density of 1 × 10^{4}cells/well and cultured for 24 h giving a 50−70% confluence. Cisplatin was then added at 0.1, 1, 10, and 100 μM concentration respectively and no cisplatin was added into control cells. The plates were incubated at 37 °C and 5% CO_2 for 48 h. Ten microliters of Alamar Blue (AbD Serotec, U.K.) was then added to each well and the plates were incubated for another 2 h before measurement. The fluorescence intensity was measured using a Victor 1402 multilabel counter (Wallac) using an excitation wavelength of 550 nm and an emission wavelength of 590 nm. The cell viability was determined by the amount of fluorescence.

DAPI Staining for Nuclear Morphology

Cells were spun onto the slides at a speed at 2000 rpm for 5 min using a Cytospin3 centrifuge (Shandon, U.K.) and stained with 0.4 μg/mL DAPI for 15 min. The slides were visualized with a Nikon Eclipse E600 microscope using 100× objective lens and images were taken using a DXM1200 digital camera with the Nikon ACT-1 software. A DAPI UV (UV-2A) filter with an excitation wavelength of 340−380 nm was used to detect DAPI stained nuclei.

RNA Extraction and Electrophoresis

To extract the total RNA from cells, 2.5 mL TRIzol Reagent (Invitrogen, U.K.) was added into one 25 cm^2 flask with cells ready to harvest. 500 μL chloroform was added to each cell lysate to achieve phase separation. The upper aqueous phase with RNA was transferred into a fresh tube and the RNA was precipitated with 1.25 mL 100% isopropanol (Sigma-Aldrich, U.K.). After being washed twice with 75% ethanol, RNA was dissolved in 30 μL RNase-free solution. One microgram of 1 Kb plus DNA Ladder (Invitrogen, U.K.) and 10 μg RNA of each sample were added on a 1% agarose gel, and electrophoresis was performed at 120 V for 90 min.

Extraction of Metabolites from Cell Preparations

Metabolite extraction was performed on all four cell lines with and without cisplatin exposure for assignment purposes. A dual phase methanol-chloroform extraction protocol was used to extract cell metabolites for ^{1}H NMR. Ten to 20 × 10^6 cells were ground and sonicated in 400 μL methanol/85 μL deionized water. Two-hundred microliters of chloroform were added to the homogenate twice to form a dual-phase. The upper water phase was collected and dried in a vacuum centrifuge at room temperature.

HR-MAS

HR-MAS was performed to measure the alteration of UDP-GlcNAc and UDP-GlaNAc with treatment. Prior to HR-MAS, frozen cells were defrosted, and 36 μL, containing approximately

dx.doi.org/10.1021/pr200114v |J. Proteome Res. XXXX, XXX, 000–000

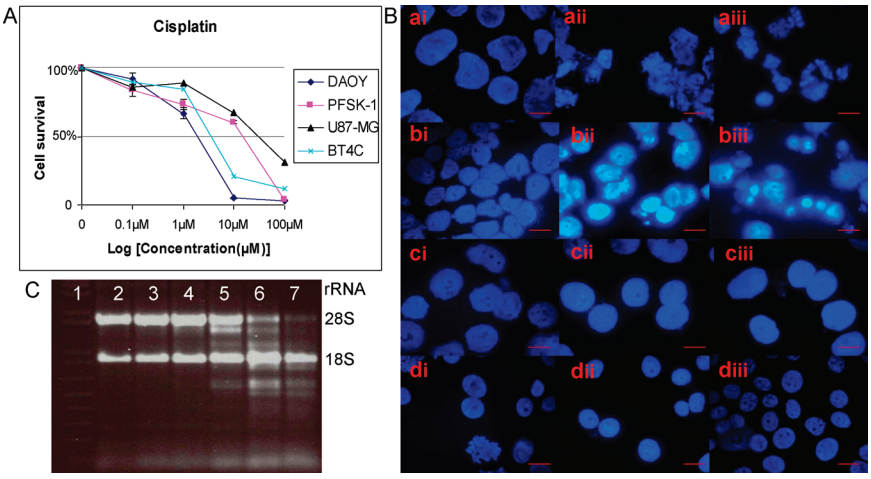

Figure 1. Cisplatin treatment of four brain tumor cell lines. (A) Cell survival curve of four brain tumor cells treated with cisplatin for 48 h at the indicated concentration. (B) DAPI-stained cell nuclei with 10 μM cisplatin treatment of DAOY (a), BT4C (b), PFSK-1 (c) and U87-MG (d) at the following exposure time: 0 h (i), 24 h (ii) and 48 h (iii). The size bar represents 10 μm. (C) Total-RNA of 50 μM cisplatin treated BT4C cells 1:1kb Plus DNA Ladder, 2: 0 h, 3−7: 3 h, 6 h, 12 h, 24 h and 48 h exposed cells.

10×10^6 cells was pipetted into a wide-mouthed zirconium sample tube (Varian Inc., Palo Alto, CA); 4 μL 10 mmol/L trimethylsilylproprionate d4 (TSP, Sigma Aldrich, Dorset, U.K.) in D_2O was added as a chemical shift standard. HR-MAS was performed on a Varian 600-MHz (14.1 T) vertical bore spectrometer using a 4-mm gHX nanoprobe (Varian NMR Inc.) with a three channel Inova console running the VNMRj software. The probe temperature was set to 0.1 °C, which equated to a temperature inside the rotor of 6.7 °C determined by calibration using the methanol method (Bruker Insturments, Inc. VT-Calibration Manual). The rotor speed was 2500 Hz in all experiments. A pulse-acquire sequence incorporating one second water presaturation pulse was used for HR-MAS. The receiver bandwidth was 7200 Hz covered with 16K complex points. A total of 256 scans were acquired with a repetition time of 3.3 s. At least three independent preparations were assessed for each time point of each cell line.

^{1}H NMR of UDP-GlcNAc and UDP-GalNAc Compounds

Dried metabolite extracts were resuspended in 600 μL D_2O containing 5 μL 10 mM TSP. Ten mM UDP-GlcNAc and UDP-GalNAc (Sigma Aldrich, Dorset, U.K.) solution was made with D_2O and the pH was adjusted to 7. Ten microliters of the compound solution was added into cell extracts for spiking experiments. ^{1}H NMR spectra of cell extracts were recorded on a Varian 600-MHz (14.1 T) vertical bore spectrometer using a HCN probe. A standard pulse-acquire sequence with water presaturation was used as above for HR-MAS.

Spectral Analysis

All spectra were manually phased. Chemical shift referencing was performed using TSP (0 ppm) for the extract spectra and creatine (3.03 ppm) for the HR-MAS spectra. Baseline correction[30] was performed and the signal intensity of the 7.85−8.05 ppm and 5.2−5.4 ppm regions were measured using integration to estimate the relative abundance of UDP-GlcNAc and UDP-GalNAc and unsaturated lipids, respectively. Signal integrals were normalized to the total intensity of the spectral region from 1.4 to 4.5 ppm as absolute concentrations were not available. Since the spectra were dominated by lipid signals at later time points an additional step of baseline correction, with increased flexibility, was performed prior to the calculation of the normalization integral. The additional baseline correction was performed to reduce the spectral contribution from increasing lipid signals that would otherwise mask the UDP-GlcNAc and UDP-GalNAc increase. The statistical total correlation spectroscopy (STOCSY) analysis method[31] was performed to aid assignment of metabolites in the HR-MAS spectra acquired. The Student's t test was performed for statistical analysis on the treated data versus the unexposed ones.

RESULTS

Cell Survival and Cell Death

The Alamar blue assay (Figure 1A) showed that the half lethal concentration (LC50) for 48 h cisplatin treatment for DAOY and BT4C cells was 1−10 μM, while the LC50 was 10−100 μM for PFSK-1 and U87-MG cells. Based on the dose−response curve, we used 10 μM cisplatin for the majority of experiments rendering DAOY and BT4C cells responders and PFSK-1 and U87-MG cells nonresponders in terms of cell death. Error bars represent standard deviation.

Nuclei of neural tumor cells (DAOY, PFSK-1) were larger than those in glioma cells (BT4C and U87-MG) prior to cisplatin treatment (Figure 1B). Interestingly, morphological changes of nuclei in responders of each cell group were much different. Nuclear fragmentation was detected in DAPI stained DAOY cells by 24 h of treatment while nuclei in PFSK-1 cells remained intact until 48 h of treatment. In BT4C cells nuclear condensation and/or swelling was evident by 48 h exposure to 10 μM-cisplatin while nuclei in U87-MG cells remained unchanged. DAOY and BT4C showed evidence for apoptosis in response to cisplatin, but PFSK-1 and U87-MG did not.

Electrophoresis of RNA extracted from cisplatin-exposed BT4C cells showed that the degradation of 28S rRNA and RNA fragments were detected by 12 h exposure to 50 μM cisplatin (Figure 1C). The RNA degradation and fragmentation increased with prolonged exposure to cisplatin.

HR-MAS Peak Assignment

The peaks at 7.98, 5.98, 5.5, and 2.09 ppm were tentatively assigned to UDP-GlcNAc and UDP-GalNAc according to the

dx.doi.org/10.1021/pr200114v |J. Proteome Res. XXXX, XXX, 000–000

literature.[10,11] The assignment was confirmed by spiking cell extracts both with pure UDP-GlcNAc and UDP-GalNAc and acquiring ^{1}H NMR (Supplementary Figure S1, Supporting Information). The STOCSY analysis of HR-MAS data from the BT4C whole cell experiments (Figure 2) showed that the peak at 2.09 ppm is correlated (R > 0.9) with the downfield peaks at around 6 and 8 ppm. STOCSY also revealed correlations for a number of other peaks, in particular one around 5.5 ppm and the region from 3.6 to 4.5 ppm. These analytic results are in good agreement with the ^{1}H NMR spectra of pure UDP-GlcNAc and UDP-GalNAc.

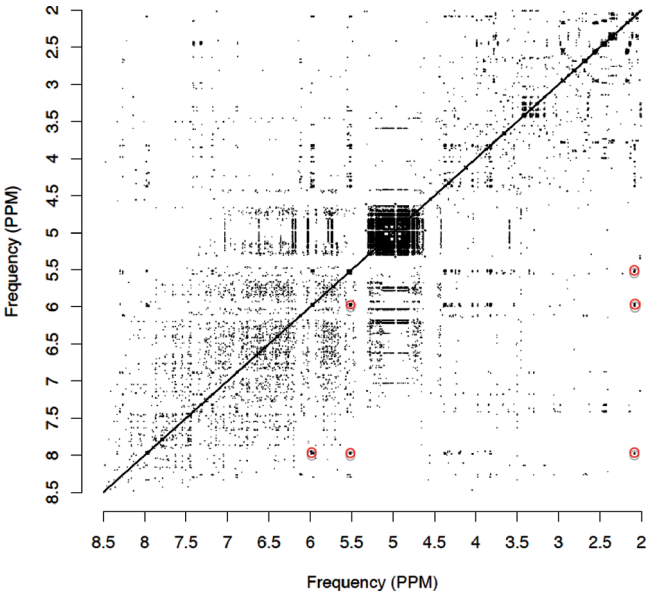

Figure 2. STOCSY analysis of all HR-MAS spectra acquired from BT4C cells. Peaks represent highly correlated spectral regions.

HR-MAS Spectral Changes in Cisplatin Exposed Tumor Cells

The HR-MAS spectra from cisplatin treated BT4C and U87-MG cells are shown in Figure 3. The HR-MAS spectra from BT4C cells showed that signal intensities of peaks at 2.09, 5.5, 5.98, and 7.98 ppm increased by 12 h and continued to further increase with time. However, in nonresponding U87-MG cells, the signals at 2.09, 5.5, 5.98, and 7.98 ppm peaks remained unchanged with cisplatin treatment.

Measurements of the 7.98 ppm peak and unsaturated lipid peak at 5.4 ppm for all cell lines are given in Figure 4 with error bars representing standard errors. The level of UDP-GlcNAc and UDP-GalNAc in untreated cells are as follows (shown in mean ± standard deviation): 0.024 ± 0.005 for DAOY, 0.006 ± 0.001 for BT4C, 0.012 ± 0.002 for PFSK-1 and 0.021 ± 0.002 for U87-MG. Large increases were shown in glycosylated UDP compounds with treatment in both of the responding cell lines

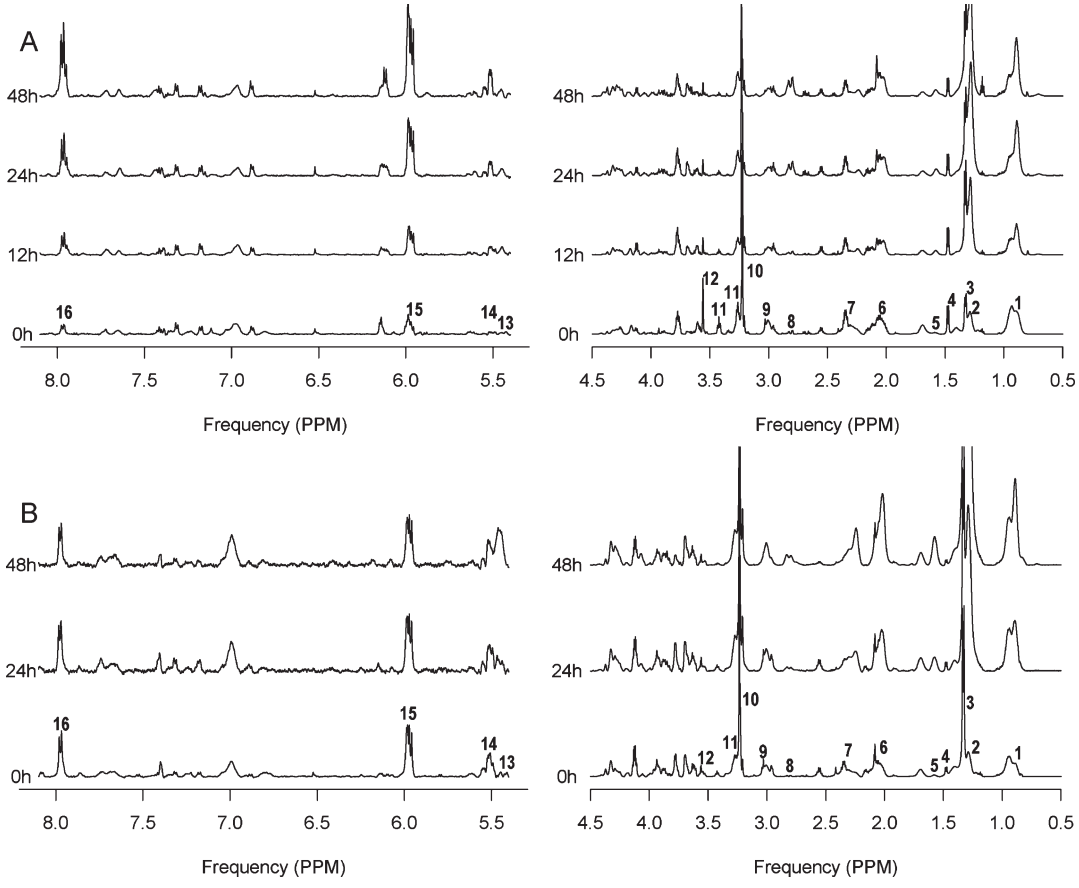

Figure 3. HR-MAS spectra of a responder and a nonresponder. (A) Cisplatin (50 μM) treated BT4C cells. (B) Cisplatin (10 μM) treated U87-MG cells. Numbers in the 0 h spectra represent the peaks as follows 1, C**H**$_3$; 2, C**H**$_2$; 3, Lactate; 4, Alanine; 5, C**H**$_2$CH$_2$CO; 6,G$_{CH3}$; 7, Glutamate; 8, =CHC**H**$_2$CH=; 9, Creatine; 10, Total choline; 11, Taurine; 12, Glycine; 13, C**H**=; 14, G$_2$ at 5.5 ppm; 15, U$_5$; 16, U$_6$. G$_{CH3}$ and G$_2$ indicate signals compatible with the −CH$_3$ and carbon 2 position of the hexose protons whereas U$_5$ and U$_6$ refer to protons on carbons 5 and 6 in the uracil ring of UDP.

dx.doi.org/10.1021/pr200114v | J. Proteome Res. XXXX, XXX, 000–000

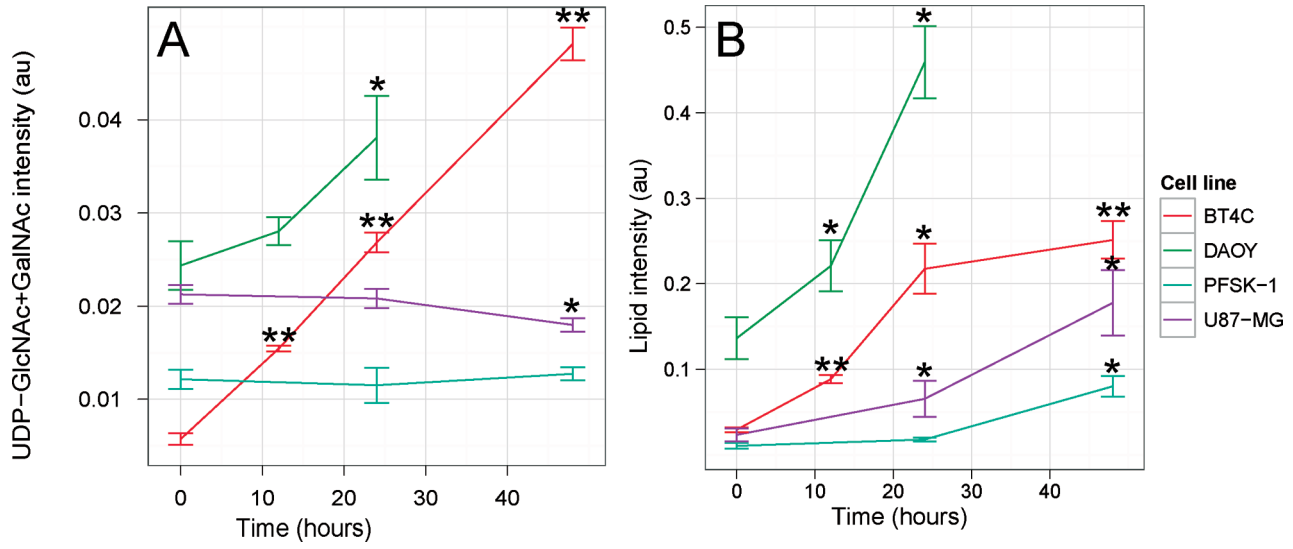

Figure 4. Measurement of HR-MAS spectra. (A) UDP-GlcNAc and UDP-GalNAc peak at 7.98 ppm. (B) Lipid peak at 5.3 ppm at 0 h, 12 h, 24 h and 48 h treatment with 10 μM cisplatin. The error bars represent standard errors. *$P < 0.05$ **$P < 0.001$.

(DAOY and BT4C) but no change in the nonresponding U87-MG and PFSK-1 cells (Figure 4A). In BT4C cells, UDP-GlcNAc and UDP-GalNAc started to increase by 12 h of exposure and continued to increase with further exposure. In DAOY cells, the concentrations of UDP-GlcNAc and UDP-GalNAc were the highest of all four cell lines prior to treatment and the increase started to show a statistical difference (Student t test, $p = 0.03$) by 24 h exposure coinciding with the initiation of morphological changes in the cell nuclei. Proton NMR-detected lipids at 5.4 ppm increased extensively with cisplatin treatment in both BT4C and DAOY cells up to 24 h (Figure 4B). There was a smaller increase in ^{1}H NMR detected lipids in U87-MG cells at 24 h but PFSK-1 cells showed no significant increase in lipids up to that time point. The lipids increased significantly in all cell lines at 48 h, and in DAOY the HR-MAS spectra acquired at 48 h were dominated by lipid peaks with hardly any metabolite peaks visible.

DISCUSSION

In tumor cells undergoing cisplatin-induced apoptosis/cell death, UDP-GlcNAc and UDP-GalNAc increase in parallel with ^{1}H NMR detectable lipids. In the cisplatin resistant cells, no increase in these two UDP-compounds was observed during exposure to the drug suggesting that the effects are due to ongoing cell death. UDP-GlcNAc and UDP-GalNAc are already implicated in cancer proliferation and malignant transformation, owing to their role in protein and lipid glycosylation. However, the current data also points to an involvement for these compounds in cancer cell death.

The most intense signals from UDP-GlcNAc and UDP-GalNAc arise in the region of the spectrum between 2 and 2.1 ppm, where the protons in the N-acetyl moieties appear as a singlet. However, this region can also be occupied by signals from glutamate and glutamine, potentially making assignment ambiguous. To confirm the correct assignment of these resonances two approaches were taken: first the aqueous fraction of cell extracts was spiked with solutions of UDP-GlcNAc and UDP-GalNAc. Signals originating from these solutions were found to be coresonant with signals present in the extract spectra (Supplementary Figure S1, Supporting Information). Second, a STOCSY analysis was performed using the HR-MAS spectra from BT4C. Strong correlations were found between the primary resonances of UDP-GlcNAc and UDP-GalNAc (Figure 2). These approaches confirm that the resonances at 2.09, 5.5, 5.98, and 7.98 ppm originate from a combination of UDP-GlcNAc and UDP-GalNAc.

Although UDP-GlcNAc and UDP-GalNAc are stereoisomers, it is still possible to differentiate between them using 1D ^{1}H NMR. From the aqueous extract data, sufficient resolution was available to distinguish between UDP-GlcNAc and UDP-GalNAc based on two well resolved resonances at 5.52 and 5.55 ppm[10] and the feature close to 2.09 ppm which had an asymmetric appearance. In all extract spectra where resonances at 2.09 ppm were visible, the peaks from UDP-GlcNAc and UDP-GalNAc were estimated to be present at a similar ratio of 3:2.

UDP-GlcNAc and UDP-GalNAc are synthesized in the cell cytoplasm and are the end products of the HBP. They are both important donor molecules for glycosylation reactions taking place in the nucleus, cytoplasm, endoplasmic reticulum or in the Golgi complex.[4,32,33] Glycosylation is a crucial post-transcriptional modification for many functional proteins, proteoglycans and lipids[2,7] determining three-dimensional structures of these macromolecules. Diabetes, cardiac myopathy and severe injury from trauma are found to be associated with transient or prolonged hyperglycemias leading to an increase of glucose uptake in mammalian cells followed with a accelerated flux in the HBP and increased protein O-glycosylation.[4,34] This indicates the important role of UDP-GlcNAc and UDP-GalNAc in cellular response to stressful conditions. Proteins involved in apoptotic pathways such as ERK, PKC and Bcl-2 have been reported to have their activity or expression levels altered in response to the increased O-GlcNAc formation.[34]

UDP-GlcNAc and UDP-GalNAc have been reported to inhibit differentiation of human colon cancer cells[35] and correlate with the degree of proliferation in malignant breast cells.[36] The level of UDP-GlcNAc was found to be a critical factor in the production of β1,6-branched oligosaccharides which have been

dx.doi.org/10.1021/pr200114v |J. Proteome Res. XXXX, XXX, 000–000

thought to be closely associated with tumor progression and metastasis.[37] In contrast, very little is known about UDP-GlcNAc and UDP-GalNAc in the response of cancer cells to treatment. Our study is the first to indicate a role for glycosylated UDPs in cancer cell death. There are some reports in the literature of O-glycosylated compounds, but not directly with glycosylated UDPs. It has been shown in colon cancer cells (HT29) that mitotic arrest by means of microtubule-destablising agents causes an increase in O-GlcNAc.[38] This compound has the N-acetyl signal, but not the UDP part seen in the low-field range of the ^{1}H NMR. Similarly, reports have been published that the N-acetyl signal from either N-acetyl groups of glycoproteins[39] or N-acetylhexoseamines[40] is detectable in vivo either in a solid tumor or cystic fluid. These studies have demonstrated the presence of O-linked acetyl compounds in cancer cells or tumors, but not indicated any specific function for these compounds.

Using HR-MAS of ex vivo specimens from untreated and HSV-tk gene therapy treated BT4C gliomas, numerous peaks in the downfield part of the spectrum were detected. These peaks were tentatively assigned as adenine, uridine and cytosine nucleotides based on the chemical shifts. The assignment of a doublet at 7.95 ppm to UDP was confirmed by spiking experiments of tumor extracts in conjunction with ^{1}H and ^{31}P NMR.[25]

The early increase in UDP-GlcNAc and UDP-GalNAc in response to cisplatin treatment response could be caused by a decrease in utilization, an increase in production or a combination of both. The degradation of 28S rRNA, a signature of apoptosis[41,42] and associated with the inhibition of protein synthesis,[43] was evident by 12 h of cisplatin treatment (Figure 1C). Under these conditions there is likely to be less protein and lipid glycosylation with a concomitant increase in UDP-GlcNAc and UDP-GalNAc. Decreased utilization of UDP-GlcNAc and UDP-GalNAc may also result directly from reduced activity of O-linked UDP-*N*-acetylglucosamine/polypeptide-*N*-acetylglucosaminyl transferase (OGT). OGT catalyzes the addition of O-GlcNAc from UDP-GlcNAc to proteins and is located predominantly within the nucleus as determined by immunofluorescence and subcellular fractionation.[7] The destruction of the nucleus after cisplatin treatment is likely to result in a decreased activity of OGT. The increase of UDP-GlcNAc and UDP-GalNAc could also be due to an increase in their synthesis. It is known that glycosylated UDPs are needed to change the antigenicity of dying cancer cells to attract macrophages for clearance of dying cells, similar to externalisation of phosphatidylserine.[44] Furthermore, UDP-GlcNAc and UDP-GalNAc levels could be elevated as a result of the increased cellular glucose uptake which is known to occur under conditions of cell stress and has been associated with an increase in their synthesis.[4,7]

Recent evidence from T98G and A172 human glioblastoma cells, indicates that cell growth arrest without cell death does not cause an increase in either UDP-GlcNAc or UDP-GalNAc.[11] We determined the level of these two metabolites in overconfluent BT4C cells and found no increase in UDP-GlcNAc or UDP-GalNAc (Supplementary Figure S3, Supporting Information). Our data indicates that UDP-GlcNAc and UDP-GalNAc are early ^{1}H NMR detectable indices of positive treatment response in brain tumor cells rather than markers of proliferation inhibition.

In our study, the increase of UDP-GlcNAc and UDP-GalNAc was found to be closely correlated with the increase in ^{1}H NMR detectable lipids in responding cells. It has previously been reported that, in the hepatic cell line HepG2, HBP flux promotes endoplasmic reticulum stress and intracellular neutral lipids accumulation.[44] In turn, the concentration of UDP-GlcNAc within cells is proposed to be modulated by the availability of fatty acids.[45,46] These observations show that there is a close association of lipid levels with hexosamine biosynthesis. The modest lipid increase in ^{1}H NMR lipids in U87-MG cells is likely to be due to the growth pattern of this cell line with focally high cell density,[29] but without effective overall growth inhibition.

In conclusion, UDP-GlcNAc and UDP-GalNAc are increased early in cancer cells which are responding to treatment and are potential candidates for treatment response monitoring by in vivo ^{1}H NMR. The observation that these glycosylated UDP compounds increase in association with ^{1}H NMR lipids may also provide mechanistic information about cell death processes, in particular to the biogenesis of lipid droplets, a hallmark process in the apoptotic cell death that renders cell lipids ^{1}H NMR detectable.

■ ASSOCIATED CONTENT

Supporting Information

Supplementary figures. This material is available free of charge via the Internet at http://pubs.acs.org.

■ AUTHOR INFORMATION

Corresponding Author

*Andrew C. Peet, Institute of Child Health, Whittall Street, Birmingham, B4 6NH, U.K. E-mail: a.peet@bham.ac.uk. Tel: 44-0121-333-8233. Fax: 44-0121-333-8241.

Author Contributions

¶These authors made equal contributions to this work

■ ACKNOWLEDGMENT

^{1}H NMR experiments were carried out in the Henry Wellcome Building for Biomolecular NMR Spectroscopy at the University of Birmingham and we are grateful for the support of the staff at this facility. The work was partly funded by the Medical Research Council, U.K. (Grant G0601327), the Andrew McCartney Trust Fund for Brain Tumour Research, Birmingham Children's Hospital Research Foundation, Poppy Fields and the Brain and Nervous System Tumour Research Fund.

■ REFERENCES

(1) Butkinaree, C.; Park, K.; Hart, G. W. O-linked beta-N-acetylglucosamine (O-GlcNAc): Extensive crosstalk with phosphorylation to regulate signaling and transcription in response to nutrients and stress. *Biochim. Biophys. Acta* **2010**, *1800* (2), 96–106.

(2) Torres, C. R.; Hart, G. W. Topography and polypeptide distribution of terminal N-acetylglucosamine residues on the surfaces of intact lymphocytes. Evidence for O-linked GlcNAc. *J. Biol. Chem.* **1984**, *259* (5), 3308–17.

(3) Copeland, R. J.; Bullen, J. W.; Hart, G. W. Cross-talk between GlcNAcylation and phosphorylation: roles in insulin resistance and glucose toxicity. *Am. J. Physiol. Endocrinol. Metab.* **2008**, *295* (1), E17–28.

(4) Zachara, N. E.; Hart, G. W. O-GlcNAc a sensor of cellular state: the role of nucleocytoplasmic glycosylation in modulating cellular function in response to nutrition and stress. *Biochim. Biophys. Acta* **2004**, *1673* (1−2), 13–28.

(5) Love, D. C.; Hanover, J. A., The hexosamine signaling pathway: deciphering the "O-GlcNAc code. *Sci. STKE* **2005**, *2005*, (312), re13.
(6) Vosseller, K.; Wells, L.; Lane, M. D.; Hart, G. W. Elevated nucleocytoplasmic glycosylation by O-GlcNAc results in insulin resistance associated with defects in Akt activation in 3T3-L1 adipocytes. *Proc. Natl. Acad. Sci. U.S.A.* **2002**, *99* (8), 5313–8.
(7) Zachara, N. E.; Hart, G. W. Cell signaling, the essential role of O-GlcNAc!. *Biochim. Biophys. Acta* **2006**, *1761* (5−6), 599–617.
(8) Gu, Y.; Mi, W.; Ge, Y.; Liu, H.; Fan, Q.; Han, C.; Yang, J.; Han, F.; Lu, X.; Yu, W. GlcNAcylation plays an essential role in breast cancer metastasis. *Cancer Res.* **2010**, *70* (15), 6344–51.
(9) Hart, G. W.; Housley, M. P.; Slawson, C. Cycling of O-linked beta-N-acetylglucosamine on nucleocytoplasmic proteins. *Nature* **2007**, *446* (7139), 1017–22.
(10) Coen, M.; Want, E. J.; Clayton, T. A.; Rhode, C. M.; Hong, Y. S.; Keun, H. C.; Cantor, G. H.; Metz, A. L.; Robertson, D. G.; Reily, M. D.; Holmes, E.; Lindon, J. C.; Nicholson, J. K. Mechanistic aspects and novel biomarkers of responder and non-responder phenotypes in galactosamine-induced hepatitis. *J. Proteome Res.* **2009**, *8* (11), 5175–87.
(11) Grande, S.; Palma, A.; Luciani, A. M.; Rosi, A.; Guidoni, L.; Viti, V. Glycosidic intermediates identified in ^{1}H MR spectra of intact tumour cells may contribute to the clarification of aspects of glycosylation pathways. *NMR Biomed.* **2010**, *24* (1), 68–79.
(12) Lindon, J. C.; Holmes, E.; Nicholson, J. K. So what's the deal with metabonomics? *Anal. Chem.* **2003**, *75* (17), 384A–391A.
(13) Mirbahai, L.; Wilson, M.; Shaw, C. S.; McConville, C.; Malcomson, R. D. G.; Griffin, J. L.; Kauppinen, R. A.; Peet, A. C. ^{1}H magnetic resonance spectroscopy metabolites as biomarkers for cell cycle arrest and cell death in rat glioma cells. *Int. J. Biochem. Cell Biol.* **2010**.
(14) Lutz, N. W. From metabolic to metabolomic NMR spectroscopy of apoptotic cells. *Metabolomics* **2005**, *1* (3), 251–268.
(15) Griffin, J. L.; Blenkiron, C.; Valonen, P. K.; Caldas, C.; Kauppinen, R. A. High-resolution magic angle spinning ^{1}H NMR spectroscopy and reverse transcription-PCR analysis of apoptosis in a rat glioma. *Anal. Chem.* **2006**, *78* (5), 1546–52.
(16) Meisamy, S.; Bolan, P. J.; Baker, E. H.; Bliss, R. L.; Gulbahce, E.; Everson, L. I.; Nelson, M. T.; Emory, T. H.; Tuttle, T. M.; Yee, D.; Garwood, M. Neoadjuvant chemotherapy of locally advanced breast cancer: predicting response with in vivo ^{1}H MR spectroscopy--a pilot study at 4 T. *Radiology* **2004**, *233* (2), 424–31.
(17) Hakumaki, J. M.; Poptani, H.; Sandmair, A. M.; Yla-Herttuala, S.; Kauppinen, R. A. ^{1}H MRS detects polyunsaturated fatty acid accumulation during gene therapy of glioma: implications for the in vivo detection of apoptosis. *Nat. Med.* **1999**, *5* (11), 1323–7.
(18) Bogin, L.; Papa, M. Z.; Polak-Charcon, S.; Degani, H. TNF-induced modulations of phospholipid metabolism in human breast cancer cells. *Biochim. Biophys. Acta* **1998**, *1392* (2−3), 217–32.
(19) Podo, F. Tumour phospholipid metabolism. *NMR Biomed.* **1999**, *12* (7), 413–39.
(20) Teichert, F.; Verschoyle, R. D.; Greaves, P.; Edwards, R. E.; Teahan, O.; Jones, D. J.; Wilson, I. D.; Farmer, P. B.; Steward, W. P.; Gant, T. W.; Gescher, A. J.; Keun, H. C. Metabolic profiling of transgenic adenocarcinoma of mouse prostate (TRAMP) tissue by 1H-NMR analysis: evidence for unusual phospholipid metabolism. *Prostate* **2008**, *68* (10), 1035–47.
(21) Lutz, N. W.; Tome, M. E.; Cozzone, P. J. Early changes in glucose and phospholipid metabolism following apoptosis induction by IFN-gamma/TNF-alpha in HT-29 cells. *FEBS Lett.* **2003**, *544* (1−3), 123–8.
(22) Nunn, A. V.; Barnard, M. L.; Bhakoo, K.; Murray, J.; Chilvers, E. J.; Bell, J. D. Characterisation of secondary metabolites associated with neutrophil apoptosis. *FEBS Lett.* **1996**, *392* (3), 295–8.
(23) Aboagye, E. O.; Bhujwalla, Z. M.; Shungu, D. C.; Glickson, J. D. Detection of tumor response to chemotherapy by 1H nuclear magnetic resonance spectroscopy: effect of 5-fluorouracil on lactate levels in radiation-induced fibrosarcoma 1 tumors. *Cancer Res.* **1998**, *58* (5), 1063–7.
(24) Zoula, S.; Rijken, P. F.; Peters, J. P.; Farion, R.; Van der Sanden, B. P.; Van der Kogel, A. J.; Decorps, M.; Remy, C. Pimonidazole binding in C6 rat brain glioma: relation with lipid droplet detection. *Br. J. Cancer* **2003**, *88* (9), 1439–44.
(25) Lehtimäki, K. K.; Valonen, P. K.; Griffin, J. L.; Väisänen, T. H.; Gröhn, O. H. J.; Kettunen, M. I.; Vepsäläinen, J.; Ylä-Herttuala, S.; Nicholson, J.; Kauppinen, R. A. Metabolite Changes in BT4C Rat Gliomas Undergoing Ganciclovir-Thymidine Kinase Gene Therapy-induced Programmed Cell Death as Studied by 1H NMR Spectroscopy in Vivo, ex Vivo, and in Vitro. *J. Biol. Chem.* **2003**, *278* (46), 45915–45923.
(26) Schmitz, J. E.; Kettunen, M. I.; Hu, D. E.; Brindle, K. M. 1H MRS-visible lipids accumulate during apoptosis of lymphoma cells in vitro and in vivo. *Magn. Reson. Med.* **2005**, *54* (1), 43–50.
(27) Blankenberg, F. G.; Storrs, R. W.; Naumovski, L.; Goralski, T.; Spielman, D. Detection of apoptotic cell death by proton nuclear magnetic resonance spectroscopy. *Blood* **1996**, *87* (5), 1951–1956.
(28) Al-Saffar, N. M. S.; Titley, J. C.; Robertson, D.; Clarke, P. A.; Jackson, L. E.; Leach, M. O.; Ronen, S. M. Apoptosis is associated with triacylglycerol accumulation in Jurkat T-cells. *Br. J. Cancer* **2002**, *86* (6), 963–970.
(29) Barba, I.; Cabanas, M. E.; Arus, C. The relationship between nuclear magnetic resonance-visible lipids, lipid droplets, and cell proliferation in cultured C6 cells. *Cancer Res.* **1999**, *59* (8), 1861–8.
(30) Xi, Y.; Rocke, D. M. Baseline correction for NMR spectroscopic metabolomics data analysis. *BMC Bioinform.* **2008**, *9*, 324.
(31) Cloarec, O.; Dumas, M.-E.; Craig, A.; Barton, R. H.; Trygg, J.; Hudson, J.; Blancher, C.; Gauguier, D.; Lindon, J. C.; Holmes, E.; Nicholson, J. Statistical Total Correlation Spectroscopy:An Exploratory Approach for Latent Biomarker Identification from Metabolic ^{1}H NMR Data Sets. *Anal. Biochem.* **2005**, *77* (5), 1282.
(32) Lau, K. S.; Partridge, E. A.; Grigorian, A.; Silvescu, C. I.; Reinhold, V. N.; Demetriou, M.; Dennis, J. W. Complex N-glycan number and degree of branching cooperate to regulate cell proliferation and differentiation. *Cell* **2007**, *129* (1), 123–34.
(33) Kolset, S. O.; Prydz, K.; Pejler, G. Intracellular proteoglycans. *Biochem. J.* **2004**, *379* (Pt 2), 217–27.
(34) Chatham, J. C.; Nöt, L. G.; Fülöp, N.; Marchase, R. B. Hexosamine Biosynthesis and Protein O-Glycosylation: the First Line of Defense Against Stress, Ischemia, and Trauma. *Shock* **2008**, *29* (4), 431–44010.1097/SHK.0b013e3181598bad.
(35) Stan-Lotter, H.; Bragg, P. D. Loss of protection by nucleotides against proteolysis and thiol modification in the isolated alpha-subunit from F1 ATPase of Escherichia coli mutant uncA401. *Biochem. J.* **1984**, *224* (1), 145–51.
(36) Slawson, C.; Pidala, J.; Potter, R. Increased N-acetyl-beta-glucosaminidase activity in primary breast carcinomas corresponds to a decrease in N-acetylglucosamine containing proteins. *Biochim. Biophys. Acta* **2001**, *1537* (2), 147–57.
(37) Sasai, K.; Ikeda, Y.; Fujii, T.; Tsuda, T.; Taniguchi, N. UDP-GlcNAc concentration is an important factor in the biosynthesis of β1,6-branched oligosaccharides: regulation based on the kinetic properties of N-acetylglucosaminyltransferase V. *Glycobiology* **2002**, *12* (2), 119–127.
(38) Haltiwanger, R. S.; Philipsberg, G. A. Mitotic Arrest with Nocodazole Induces Selective Changes in the Level of O-Linked N-Acetylglucosamine and Accumulation of Incompletely Processed N-Glycans on Proteins from HT29 Cells. *J. Biol. Chem.* **1997**, *272* (13), 8752–8758.
(39) Kolwijck, E.; Engelke, U. F.; van der Graaf, M.; Heerschap, A.; Blom, H. J.; Hadfoune, M.; Buurman, W. A.; Massuger, L. F.; Wevers, R. A. N-acetyl resonances in in vivo and in vitro NMR spectroscopy of cystic ovarian tumors. *NMR Biomed.* **2009**, *22* (10), 1093.
(40) Santhosh, K.; Thomas, B.; Varma, L.; Sandhyamany, S.; Kesavadas, C.; Appukuttan, P.; Srinivas, G.; Gupta, A. K.; Kapilamoorthy, T.; Unnikrishnan, M. Metabolite signature of developmental foregut cyst on in vivo and in vitro ^{1}H MR spectroscopy. *J. Magn. Reson. Imaging* **2008**, *28* (2), 493.

(41) Samali, A.; Gilje, B.; Doskeland, S. O.; Cotter, T. G.; Houge, G. The ability to cleave 28S ribosomal RNA during apoptosis is a cell-type dependent trait unrelated to DNA fragmentation. *Cell Death Differ.* **1997**, *4* (4), 289–93.

(42) King, K. L.; Jewell, C. M.; Bortner, C. D.; Cidlowski, J. A. 28S ribosome degradation in lymphoid cell apoptosis: evidence for caspase and Bcl-2-dependent and -independent pathways. *Cell Death Differ.* **2000**, *7* (10), 994–1001.

(43) Nadano, D.; Sato, T.-A. Caspase-3-dependent and -independent Degradation of 28 S Ribosomal RNA May Be Involved in the Inhibition of Protein Synthesis during Apoptosis Initiated by Death Receptor Engagement. *J. Biol. Chem.* **2000**, *275* (18), 13967–13973.

(44) Sage, A. T.; Walter, L. A.; Shi, Y.; Khan, M. I.; Kaneto, H.; Capretta, A.; Werstuck, G. H. Hexosamine biosynthesis pathway flux promotes endoplasmic reticulum stress, lipid accumulation, and inflammatory gene expression in hepatic cells. *Am. J. Physiol. Endocrinol. Metab.* **2010**, *298* (3), E499–511.

(45) Wells, L.; Vosseller, K.; Hart, G. W. A role for N-acetylglucosamine as a nutrient sensor and mediator of insulin resistance. *Cell. Mol. Life Sci.* **2003**, *60* (2), 222–8.

(46) Hawkins, M.; Barzilai, N.; Liu, R.; Hu, M.; Chen, W.; Rossetti, L. Role of the glucosamine pathway in fat-induced insulin resistance. *J. Clin. Invest.* **1997**, *99* (9), 2173–82.